Asian Journal of Chemistry; Vol. 34, No. 12 (2022), 3048-3058

ASIAN JOURNAL OF CHEMISTRY

https://doi.org/10.14233/ajchem.2022.24044

REVIEW

Synthesis, Characterization and Applications of Plain and Non-Metal Doped, Biomass-Derived Carbon Quantum Dots: A Short Review

A. PADMAPRIYA[1], R. KRISHNAVENI[2,*], R.A. KALAIVANI[1,*] and A.M. SHANMUGHARAJ[3]

[1]Department of Chemistry, Vels Institute of Science, Technology and Advanced Studies, Chennai-600117, India
[2]Saveetha School of Engineering, Saveetha Institute of Medical and Technical Sciences (SIMATS), Thandalam, Chennai-602105, India
[3]Centre for Energy and Alternative Fuels, Department of Chemistry, Vels Institute of Science, Technology and Advanced Studies, Chennai-600117, India

*Corresponding authors: E-mail: krishflowers@gmail.com; rakvani@yahoo.co.in

Received: 19 September 2022; *Accepted*: 10 October 2022; *Published online*: 25 November 2022; AJC-21027

Carbon dots (CDs) are very small particles have acquired research interest in the last few years, due to their unique characteristics like low-cost synthetic protocols, fast and flexible modification procedures and low toxicity. These CDs exhibit excellent physical and chemical properties like high crystallization, superconductivity, electronic conductivity, *etc.* and hence they establish themselves as massive entrants in emerging fields of applications like chemical sensors, nanomedicines and electrocatalytic reactions. Functional nanosensors with luminescent properties are in high demand in bioanalysis and doped carbon dots play a great role in this feature. The elements *viz.* B, C, N, P and S doped carbon dots are used in the detection of metal ions in biological samples, bioimaging and DNA studies. This critical review examines the environmentally friendly techniques of synthesizing doped/undoped carbon quantum dots from biomasses, with an emphasis on their electrochemical and luminescent applications.

Keywords: Carbon quantum dots, Doped quantum dots, Biomass, Sensors.

INTRODUCTION

Quantum dots (QDs) are the zero-dimensional nano-materials with diameters in the range of 1-10 nm and are the most deeply researched materials having an incredible application values. Owing to their quantine confinement, they exhibit unique optical, photocatalytic and semiconductor properties [1]. Carbon quantum dots (CQDs), primarily obtained from the naturally occurring resources, provide ventures in the designing and creation of new devices with interesting properties and functions [2-5]. CQDs stand out as a novel and promising fluorescent carbon material, because of their special optical properties, great water solvency, high security, low toxicity fantastic biocompatibility and low ecological effects [6]. Carbon dots are highly appealing in a variety of applications due to their remarkable optical and electrical capabilities as well as their cost-effective and non-toxic features. For example, biosensors, opto-electronic gadgets, catalysts,bioimaging and labeling [7]. Further, fine-tuning and specifications of CQDs are achieved by doping and numerous state-of-the-art techniques like electrochemical and ultrasonic methods, hydrothermal, arc-discharge and laser ablation have been already reported in this context [8-12]. Apart from cellular imaging and drug delivery of CQDs, fluorescent properties of elements N, P and S doped CQDs find wide applications as photocatalysts [13] and fluore-scent inks in identifying many metallic ions [14,15] like Hg^{2+}, Fe^{3+}, Zn^{2+}, Cu^{2+}, Eu^{3+} and As^{3+}. Detection of organic samples including pesticides and *N*-containing drugs like glutathione, methimazole, *etc.* are also reported [16-18]. Sensing characteristics of such CQDs modified with heteroatoms are reported to overcome the limitations often encountered with conventional organic dyes like the requirement of covalent interactions and geometric constraints (PET, ICT, MLCT, FRET mechanisms) [19-22]. On the contrary, doped CQDs operate on the inner filter effect (IFE) mechanism, which just requires the spectral overlap of the absorption band of the target metallic ion and the excitation/emission band of fluorophore

[23,24] and hence provides a simple and easy methodology for designing a fluorophore [25].

Carbon dots (CDs) and their derivatives, considered to be highly convenient and ecofriendly, can be obtained from any material containing carbon. Traditionally, CQDs are obtained from non-renewable sources such as coal, petroleum coke, sugars, *etc.* and more recently, they are prepared from biomass wastes like agricultural and food residues, livestock [26-30] municipal solid waste, *etc.* owing to their rich carbon content (45-55 wt.%) [31,32]. Fabrication of carbon dots is still in the early stage of its development, especially on having control over the size and shape of the material. The most widely followed methods like top-down (arc discharge, laser ablation, electrochemical oxidation, *etc.*) and bottom-up approaches (microwave, solvothermal, ultrasonic, pyrolysis, *etc.*) have their own advantages and disadvantages reported [33]. In such a scenario, successful and scalable methods of green synthesis of carbon quantum dots are highly appreciated. The usage of less expensive and toxic-free raw materials, renewable resources, simple operations and environmentally friendly byproducts are the main advantages of such green methods. Hence, natural biomass is highly cherished as a source of raw material for the synthesis of CQDs [34]. Methods of green synthesis of fluorescent carbon quantum dots from biomass resources like parts of plants, fruits and fruit peels, vegetables, beverages, spices, animal and human derivatives and natural polymers are available in the literature [35]. Methods like hydrothermal, solvothermal, microwave-assisted polymerization, pyrolysis, carbonization are mostly used in fabricating quantum carbon dots [36]. Interestingly, many doped carbon dots obtained from natural biomass sources are found to be fluorescent and hence can be widely used for metal ion sensing and cell imaging studies. For instance, highly blue-emitting N, S co-doped CDs were prepared from onion and bean pods by simple hydrothermal treatments [37]. Similar fluorescent CDs are also reported to be obtained from precursors like ginger [38], papaya [39], lemon juice [40], bee pollens [41] , sweet pepper [42], *etc*. Several spectroscopic techniques like UV-Vis, IR, Raman, XPS, TEM, *etc*. are used to characterize the carbon dots obtained by different procedures to affirm their sizes, stabilities and functionalities and the popular ones are as shown in Fig. 1.

In the following sections, a short review of the methods of synthesis of CQDs and doped CQDs from biomass resources along with their characterization techniques and applications is discussed.

Synthesis of CQDs: Synthesis of biomass-derived carbon dots (BCDs) is based on the strategic breaking down of bigger carbon resource materials (top-down) or assembling of smaller precursor materials (bottom-up). The former method involves the sizing down of particles by oxidation and reduction and/or physical grinding. Generally, the latter method has an improved yield and is mostly preferred for the reason that it is feasible to introduce heteroatoms during the synthesis itself and hence doping is successful [43]. Hitherto, various methodologies for preparing CDs from biomasses have been developed, however, the method of interest prefers to obtain BCDs using simple and modest ones which would be of low cost, helps in controlling the sizes and provides large-scale possibilities. In the above context, hydrothermal carbonization is the most common method as compared to microwave hydrothermal and microwave.

Hydrothermal carbonization (HTC): HTC is a method of high potential for producing novel carbon materials from a wide variety of biomass resources, which can be both organic and inorganic carbon sources. This is usually carried out in a stainless steel autoclave with a Teflon liner. At high temperatures and pressure under inert conditions, in the presence of water, the biomass breaks down thermochemically. Fruits, plant leaves, vegetable peels, *etc.* are successfully subjected to this method for the BCD synthesis. Lu *et al.* [44] utilized pomelo peel to synthesize water-soluble C-dots for the selective and sensitive determination of Hg^{2+} by hydrothermal method. The yield of BCDs was 6.9%. BCDs from bamboo waste were synthesized by Liu *et al*. [45] with a quantum yield of 7.1% and coated the C-dots with branched polyethyleneimine through electrostatic adsorption for the selective and sensitive detection of Cu^{2+} in river water. Food, beverage and combustion wastes were utilized as the resources to obtain multicoloured and highly luminescent CDs, which are further used in the fabrication of LEDs [46,47]. A few naturally derived BCDs are detailed in Table-1.

Further, N-doped chitosan based CQDs were recently fabricated from renewable chitosan and biocompatible amino acids by this technique [48]. Similarly, the synthesis of hydrophilic N-doped CQDs from dwarf banana peels was reported by Atchudhan *et al.* [49]. Interestingly, multiple colour emissive CQDs were reported by Gao *et al* [50], where *o*-phenylene diamine and DMF were used as precursors and thiourea was used as the S dopant to the CDs. A very simple hydrothermal carbonization technique was reported by Peng *et al.* [51] for preparing B-doped CQDs with citric acid and diboronyethane (DBE), which is found to be highly photostable and non-toxic.

Literature are also available where doping of such heteroatoms to the BCDs greatly influences the photoluminescent properties of such CDs and hence are of great interest. For example, Saengsrichan *et al*. [52] reported the extraction of CDs from the empty fruit bunch (EFB) of the palm, which was used as the precursor for preparing BCDs by hydrothermal synthetic procedure and the obtained product was found to exhibit excellent photoluminescence. Further modification of the BCDs on the surface was carried out for enhancing the photoluminescence characteristics. Many doping agents like urea, thiosulphate, sulphur, *p*-phenylenediamine were used to introduce N and/or S on the surface out of which the co-doping of *p*-phenelyenediamine and sodium thiosulphate *i.e.*, N, S doped BCDs exhibited maximum enhancement in photoluminescence behaviours. Likewise, synthesis of N, P co-doped CDs and their energy transfer studies have been reported by Yang *et al.* [53], using a FRET-based green fluorescent N, P-CQDs potential sensing determination of carbendazim.

Microwave hydrothermal method: Though not very popular, microwave-assisted synthesis of BCDs has also been widely reported. Eggshell membranes [54], coconut water [55], goose feathers [56] and more materials have been used as precursors in such procedures. A microwave is used to heat water, which reduces the reaction time. Usually, in a fast single-step hydrothermal synthesis assisted with a microwave, a

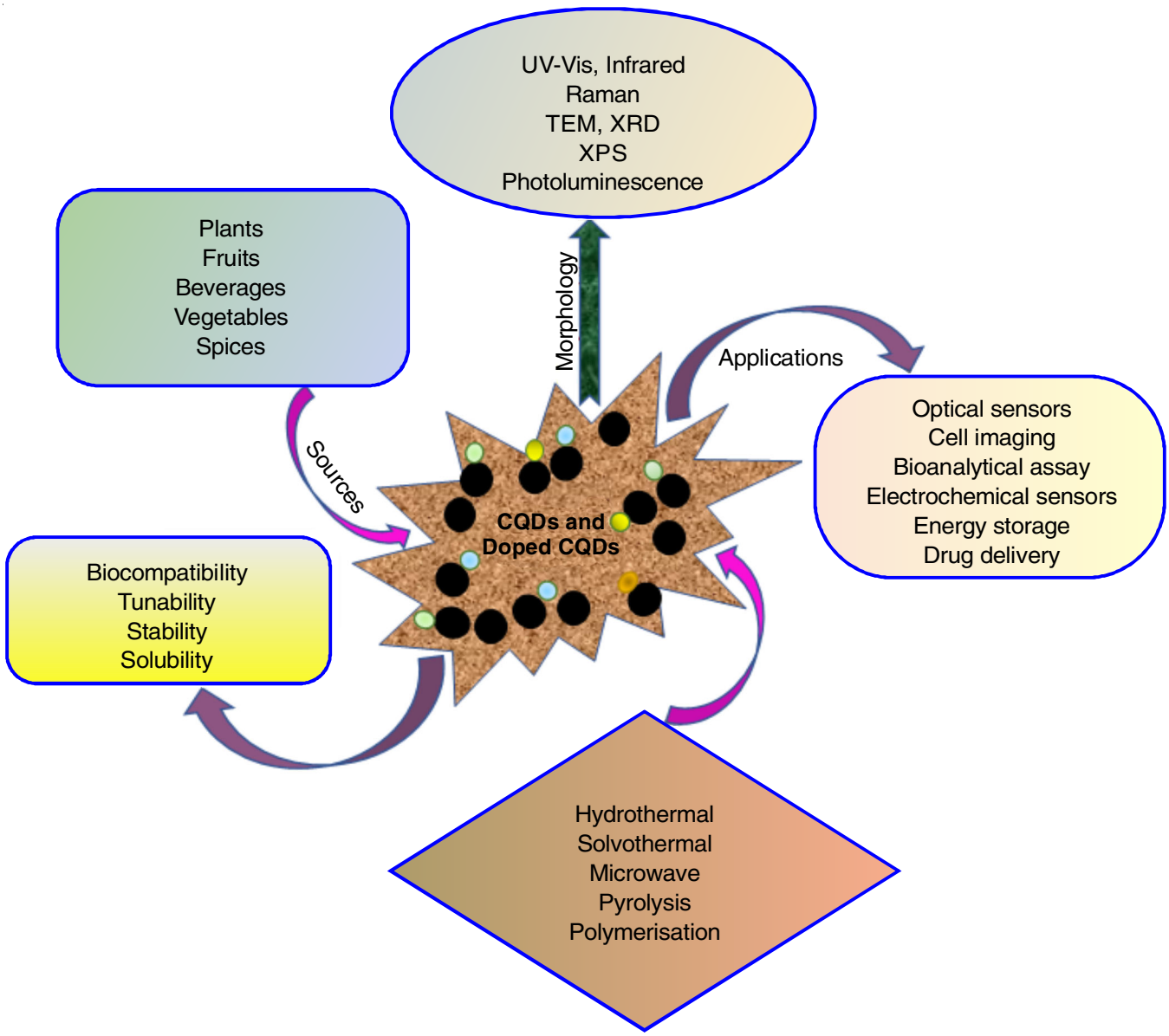

Fig. 1. Sources, methods of synthesis, properties, characterization techniques and applications of CQDs and doped CQDs

TABLE-1
DETAILS OF SYNTHESIS, QUANTUM YIELD AND APPLICATIONS OF BCDs OBTAINED FROM NATURAL CARBON RESOURCES

Source	Method	Size (nm)	Quantum yield (%)	Application	Ref.
Onion	Hydrothermal	9	28	Bio-imaging	[37]
Ginger	Hydrothermal	8.2	13.4	Bio-imaging	[38]
Papaya	Hydrothermal	3.4	19	Detecting Fe^{3+}	[39]
Lemon juice	Hydrothermal	4.6	28	Bio-imaging	[40]
Bee Pollens	Hydrothermal	1	6-12	Bio-imaging catalyst	[41]
Sweet Pepper	Hydrothermal	2-7	19.3	Detecting ClO^-	[42]
Willow bark	Hydrothermal	1-4	6	Biosensor photocatalyst	[43]
Grass	Hydrothermal	3-5	2-6	Solar cells	[43]
Pomelo peel	Hydrothermal	3	7	Detecting Hg^{2+}	[44]
Bamboo leaves	Hydrothermal	2-6	7.1	Detecting Cu^{2+}	[45]
Winter melon	Hydrothermal	4.5	7.1	Bio-imaging	[47]
Egg shell membrane	Microwave hydrothermal	5	14	Biosensor	[54]
Coconut water	Microwave hydrothermal	1-6	54	Detecting Cu^{2+}	[55]
Goose feathers	Microwave hydrothermal	21	17	Detecting Fe^{2+}	[56]
Serum albumin	Microwave	24	14	Detecting Pb^{2+}	[60]
Rose	Microwave	4-6	13.5	Detecting molecules	[62]
Eutrophic algae	Microwave	8	13	Bioimaging	[63]

digestion chamber is used, where the temperature can be monitored and controlled using the fiber optics. The pressure is maintained using a transducer connected to a reference vessel [57]. Water soluble, photoluminescent BCDs have been successfully prepared by this method and the influence of temperature over the particle size of the BCDs has been reported. For instance, from coconut water, at 140 ºC, the particle size of BCDs was 2 nm whereas at 180 ºC it was 4 nm. However, with goose feathers, particles of sizes as large as 21 nm have been reported at 180 ºC and were found to be rich in potential functional groups like N, S and O and also displayed a high quantum yield of 17.1% [56]. Tian *et al.* [58] compared the reaction timings and particle sizes of the BCDs with and without microwave assistance of the hydrothermal treatment. An evident shortening of the duration of synthesis and more uniformity in the size and shape of CDs, which provided a more conducive room for biological applications were also reported [59]. Nevertheless, the microwave hydrothermal method is not commonly used like the hydrothermal method for synthesizing BCDs. This may be due to the restricted penetration depth of microwave irradiation into absorbing materials.

Microwave method: Microwave radiation has been used more often, but the frequencies used are much lower than that in hydrothermal radiation for the synthesis of BCDs. More reports of microwave synthesis of BCDs and doped BCDs are available in the literature. To name a few are bovine serum albumin [60], flour [61], rose [62]. Synthesis of photoluminescent CQDs from eutrophic algae by simple and less toxic methodologies that use microwave energy has also been reported [63]. The main advantage of the microwave synthesis method includes rapid and uniform heating, energy-saving process, shorter preparation time, higher yields, small and narrow particle size distribution and comparatively high purity of the products. A very precise particle dimension in the range of 2-6 nm was obtained and the variation of particle sizes, from an individual source, was limited to a spectrum of 1-3 nm maximum. Reduced concentration of the reactants and raised temperatures were found to impact the control in sizes when compared to conventional procedures.

The photoluminescent properties of the precursors were intact even after the size reduction and found to exhibit substantial quantum yields in the range of 5% to 15%. Recently, CDs synthesized from palm kernel shell by microwave irradiation method have been investigated for their physical and optical applications. The highest quantum yield of 44% was observed for an irradiation period of 60 s. Hence, these material finds great application in biological cell imaging and acts as a great sensor for detecting heavy metal ions [64]. This method is also very successful in doping heteroatoms to biomass derived CDs. A very similar facile and economical green synthesis of N-doped CDs derived from a natural material *e.g.* kelp [65], which was found to be fluorescent, pH-sensitive and selective for Co(III) ions. Brilliant colour transitions of this N-doped BCD (from colourless to brownish yellow under visible and bright blue to dark blue under UV light) with a detection limit of 0.39 µmol/L, make it highly appreciable in real-time analysis of river water samples. Zhi *et al.* [66] reported the doping of phosphorous using citric acid or malic acid as carbon precursor. Such N, P co-doped materials exhibited more photostability than the N-doped ones. They were also tested for bacterial toxicity and found to be highly ecofriendly fluorescent materials. Single step microwave radiation assisted methods used for the synthesis of NP-CQD, N-CQD and P-CQD are also reported [67]. Enhanced photocatalytic activity of N, P co-doped CDs over those of N-CDs and P-CDs were also illustrated.

Characterization techniques: Since the discovery of carbon dots in 2004 and continuously explored due to their versatile properties, and extended applications. Especially, the fluorescent carbon quantum dots seem to be very interesting owing to their tunable optical properties and particle sizes. Lately, synthesis and applications of such fluorescent CDs are in a rapid pace due to the development of effortless doping strategies, their high quantum yields and applications in diverse fields. In particular, N-doped CDs display potential analytical and biological applications and hence are being widely investigated. Effective characterization becomes mandatory for predicting the applications of such molecules. In the following section, basic characterization techniques used to study the morphology and properties of carbon quantum dots and their doped derivatives are discussed.

UV-visible, FTIR and XPS characterizations: Generally, the luminescence of CDs can be understood by following their UV-vis spectroscopic absorption and fluorescence behaviours. They have strong and broad absorption bands in the visible region due to the presence of C=C, C=N bonds and C=O bonds. The possibilities of electronic transitions and hence their colour-changing properties can be extensively probed by this technique. A $\pi \rightarrow \pi^*$ transition from the ethylene group appears between 220-270 nm and that for the carboxyl group ($n \rightarrow \pi^*$ transition) appears between 280-350 nm. In addition, if peaks are observed in the range of 350 to 600 nm, it may be attributed to other functional groups on the surface of the CDs [68]. For example, a typical UV-vis absorption and emission spectra of BCDs derived from coriander leaves [69]. As far as the fluorescence of BCDs is concerned, the maxima of excitation and emission were recorded at 380 and 420 nm, respectively [70]. Further investigations of the fluorescence behaviour revealed that the wavelength maximum and intensity of emission of BCDs are highly dependent on the excitation wavelength and the behaviour is directly related to the sizes and shapes of the nanoparticles on the surface.

Not much of a difference was observed between doped and undoped BCDs as far as optical characterizations concerned. For instance, in boron-doped CDs, the $\pi \rightarrow \pi^*$ and $n \rightarrow \pi^*$ transitions of the C=C and C=O bonds present in the conjugate structures of doped CDs are represented by the two distinct peaks, at 241 and 353 nm, respectively [71,72]. As inferred from the IR spectrum of the doped CDs, the molecule displays the presence of functional groups like OH and NH in the region of 3377-3250 cm^{-1}, CH at 2916 cm^{-1}, C=O at 1648 cm^{-1}, C=C at 1569 cm^{-1}, C–H at 1393 cm^{-1}, C–O at 1013 cm^{-1} and O–H at 948 cm^{-1} [72,73].

The XPS is a powerful technique used in the characterization of carbon dots because it not only shows what elements

are present but also what other elements they are bonded to. A typical X-ray photoelectron (XPS) spectrum is a plot of the number of electrons detected at a specific binding energy. Each element produces a set of characteristic XPS peaks. These peaks correspond to the electron configuration of the electrons within the atoms, *e.g.* 1*s*, 2*s*, 2*p*, 3*s*, *etc*. The number of detected electrons in each peak is directly related to the number of elements within the XPS sampling volume [51]. The detection limit of the study is usually in parts per thousand, but can also be carried out on the scale of parts per million (ppm) with long collection times. Hence, this method proves to be very handy in the identification of functional groups and elements of BCDs, which are very tiny in structure and less in mass and concentrations.

Raman characterization: Typically, the D-band at 1385 cm^{-1} and G-band at 1575 cm^{-1} are used to study low dimensional carbon materials like graphene, nanotubes, carbon dots, *etc*. A strong G peak is usually attributed to a highly crystalline carbon structure (sp^2) as with graphene sheets [74] whereas the D band may be assigned to either a crystalline structure with defects or impurities [75] or with sp^3 hybridized carbons [76,77]. Saengsrichan *et al*. [52] demonstrated the influence of N and S doping on the structure of CDs obtained from empty fruit bunch of palm using the Raman technique. The I_D/I_G ratio for high concentrations of N and S dopants was in the range of 0.43 to 0.73. This numerical value was very similar to the I_D/I_G of graphene quantum dots that exist in 1-3 layers recorded as 0.9 [78,79]. Such a comparison reveals that the much desired property of CDs, namely, the crystallinity of BCDs obtained by doping is on par with that of graphene quantum dots due to sp^2 carbons [80], which are appreciable.

TEM & XRD techniques: The microstructure of a variety of CDs and BCDs is successfully carried out by combining these two methods. For example, the N doped CDs obtained from highland barley, Han *et al.* [81] reported the TEM and XRD spectra, wherein a uniform spherical morphology was obtained and the sizes were measured to be in the range of 4.5 to 7 nm on an average of 50 particles. A lattice spacing of 0.39 nm was revealed by the high-resolution transmission electron microscopy (HRTEM) image indicated the amorphous nature of the doped CDs. A broad X-ray diffraction peak with a peak at $2\theta = 19.96^{\circ}$ and an interlayer distance of 0.44 nm obtained further confirmed the amorphous nature of the N-doped CDs.

Similar amorphous CDs were derived from food caramels and orange peel wastes. There were no peaks observed in the XRD pattern and hence were declared as non-crystalline [82]. However, crystalline BCDs were obtained from banana peels having a particle size of 3 nm, which are spherical in shape and contain carbon, oxygen and potassium [83]. The interlayer distancing of carbon containing oxygen groups and carbon containing hydroxyl groups was found to be 0.43 nm, which is greater than that of graphite layers. When compared to crystalline CDs, amorphous ones are less explored due to the greater structural specifications and luminescence properties. However, amorphous CDs have more benefits like solubility in aqueous solutions, biocompatible nature, ease to synthesize and inexpensive. Recent explorations have established that the properties of amorphous CDs are no way inferior to their crystalline counterpart and are almost similar in all attributes including photoluminescence [84]. Interestingly, a complete understanding of the mechanism of photoluminescence from these two forms of CDs is still under active research.

Applications: Small size, excellent fluorescence intensity and good photostability, low toxicity and high biocompatibility, water solubility and superior stability and the scope for surface modification and functionalization are some exceptional properties of CQDs derived from biomasses. Obviously, these biomass derived CQDs attract lots of exploration for being used in areas like sensing analytes, *in vivo* imaging, drug delivery, photocatalysis, energy storage, light-emitting diodes, fluorescent inks, *etc*. In line with conventional CDs, many biomass-derived carbon quantum dots and their doped derivatives fit into all such optical/electronics, electrical/electronics and chemical/biological applications along with the advantage of being environmentally friendly, less toxic and inexpensive. Selected applications of such BCDs and doped derivatives are reviewed and discussed as follows:

Optical sensors: Fluorescent carbon quantum dots acquire a huge interest in recent times as optical sensors due to their excellent optical properties. As sensors, many of them are found to exhibit good selectivity and good accuracy in sensing varieties of analytes like metal ions, pharmaceutical drugs, food products, real-time soil and water samplings in river beds, *etc*. [85].

Sensors for metal ions: Doped/co-doped CDs behave as quality sensors by exhibiting colour changes with respect to the presence of many samples *viz.* metal ions like Fe^{3+}, Li^{3+}, Cr^{6+}, Hg^{2+}, Cd^{4+}, drugs like ascorbic acid, caffeine, dopamine, hydrogen peroxide and also pesticides [86]. Though mechanisms like photoinduced electron transfer (PET), fluorescence resonance energy transfer (FRET), fluorescence "On/Off", intramolecular charge transfer (ICT), metal-ligand charge transfer (MLCT), inner filter effect (IFE), ratio metric response are proposed to operate behind the sensing action of optical sensors for different probe/analyte combinations, the fluorescence on/off method and IFE methods are found to be more operating in case of CQDs for easy detection of targets [87].

The selective and sensitive detection of Fe^{3+} in water samples using N-doped CQDs as fluorescence sensors are reported by Lv *et al.* [88]. The presence of various metals like Na, K, Co, Cd, Li, Pb, Cr and Fe was successfully detected by following the fluorescence quenching and the detection limit was as low as 0.079 μM. A similar, quenching based detection of Fe^{3+} in water samples using BCDs, down to the level of 3.1 nM was reported by Jana *et al.* [89]. A very sensitive photoluminescence detection of Fe^{3+} in presence of multiple ions is also reported using N/P co-doped CQD, which was obtained from a cheap, green and edible fruit called *Eleocharis dulcis* [90]. In addition to detecting Fe^{3+}, these naturally derived CQDs exhibit high photostability and quantum yield and have a potential application to be used as fluorescent ink, multicolour imaging, fabrication of sensing devices and anticounter feiting studies.

CQDs derived from cellulose as the precursor have been reported as being used for the detection of Hg^{2+} ions [91].

Mercurous ions in combination with CQDs undergo fluorescence quenching and the mechanism is proposed as excited state electron transfer, which happens on the surface of CDs [90,92]. This product can be used for the detection of inorganic mercury in drugs, fish and other biological products, especially those with limited and strict mercury regulations [93]. Also, the detection of Cu(III) ions acquires importance in the marine ecosystems and human body. CDs obtained from bamboo biochar were found to exhibit a bright blue emission at 450 nm, which is substantially quenched by Cu(III) ions. The LOD (limit of detection) in water media is reported as 115 nm. This was also found to be a selective quenching in the presence of other ions of many other metals like, Co, Ca, Ni, Mn, Hg, Pb, Ba and Cd and hence is appreciated as an effective Cu(III) detection tool [45].

Another metal ion that is found to be quite dangerous to human health is Al(III). Hence, the detection and monitoring of Al in water and biological systems is also a relevant task that is successfully accomplished using BCDs. CDs derived from waste pears by the hydrothermal method were found to show an emission maximum at 470 nm and the particle size was 2 nm [94]. When treated with water with contamination, Al(III) ions were reported to form a chelating complex with the BCD and were found to show an irreversible quenching of the emission intensity. Again, the phenomenon was very selective to aluminum in presence of many other metallic cations, anions and varieties of organic species and the detection were possible down to the level of 2.5 nM concentration. Similarly, BCDs derived from purple perilla by hydrothermal followed by sonication methods showed an astounding LOD for Ag(I) up to 1.4 nM [38]. Likewise, BCDs obtained by microwave methods were used in detecting As(III) [95] and Fe(III) [96].

Biosensors for drugs: Other than metal ions, biomass-derived carbon dots were also used to detect many drugs and pharmaceutical molecules. For instance, tetrazine is a very popular synthetic food colorants and is widely used. Quantitative detection of this molecule in the range of 0.25 to 32.5 μM was reported by Xu *et al.* [97].

A successful On/Off fluorescence probe for the detection of curcumin in water was fabricated by Han *et al.* [98] using hydrothermal method, prepared an N and S doped CD with a high quantum yield of 26% which was successfully quenched when curcumin was introduced into the solution. The range of detection was reported as 0.15-0.18 μmol/L and LoD was 0.04 μmol/L. Additionally, this product was used for the detection of curcumin in urine samples and hence established as a successful detection tool for curcumin-based drugs in a wide variety of samples. BCDs obtained from linseed were used as a biosensor for detecting butyrylcholinesterase (BChE) [99]. A newer gas detection method based on a fluorescence quenching mechanism was successful down to the detection level of 0.035 mU mL^{-1}. Also, a FRET-based highly selective/sensitive detection tool for an anti-cancer drug called methotrexate was formulated by Wang *et al.* [100]. This method has a detection range of 50 μM and LoD of 0.33 nM and the main advantage of the method is that it can also be used in human serum. Very recently, a CQD synthesized from a natural biomass precursor *Rosa roxburghii* is reported to be used successfully for the selective detection of *o*-nitrophenol in river water and sewerage samples by Zhang *et al*. [101]. The significance is that the presence of nitroaromatics in water samples is of great environmental concern. However, the BCQD derived is reported to display high sensitivity and specificity with the detection range as 0.08-40 μmol/L and LoD as 15.2 nmol/L. In addition, the usage of this material as a nanoprobe for high-resolution imaging analysis of Hep3B cells and human hepatocellular carcinoma cells.

Detection of pesticides and fungicides: As discussed earlier, carbendazim is one such toxic broad-spectrum fungicide that is fatal even in very low doses. An operative method to detect and monitor the levels of carbendazim using an N, P co-doped carbon dots has been reported [53]. Under the optimal conditions, a linear range of detection from 0.005 μM to 0.16 μM was obtained, with a low detection limit of 0.002 μM (3δ/S) which was highly appreciable [102]. Also, an ionic-based sensor which is N, S co-doped CD for pesticide 'carbaryl' was reported by Li *et al.* [103]. In presence of other enzymes like acetylcholinesterase (AChE) and choline oxidase (ChOx), carbaryl pesticide molecules could be selectively detected with an LOD of 5.4×10^{-9} g/L and for a concentration range of 6.9×10^{-9} g/L to 6.3×10^{-9} g/L.

Electrochemical applications: By virtue of their chemical stability and inertness, tunable photoluminescence and high surface area open for modification, CQDs are offering promising methodologies to be tried out to overcome the existing challenges in energy conversion and environmental impacts. In particular, CQDs with doped heteroatoms provide desirable active sites, which enhance the electrochemiluminescence (ECL) properties. In this section, some doped/undoped QDs with electrochemical properties and their applications in sensing studies and energy storage are discussed.

Electrochemical luminescence: Electrochemiluminescence (ECL) is an interesting phenomenon in which the emission of light occurs due to the energetic electron transfer amongst the electrogenerated reactive intermediates during a potential scan [104-106]. Analytically, the system setup is optimized and shows high sensitivity and very low background signals [107, 108]. The operating mechanism is a co-reactant one and hence can be carried out both in aqueous and non-aqueous electrolyte media. Though semiconducting nanomaterials (QDs) like CdTe, CdSe/ZnS, *etc*. are already established luminophores with remarkable ECL properties, they are toxic due to the presence of heavy metal ions. Hence, carbon-based quantum dots (CQDs) and graphene quantum dots (GQDs), which are less toxic and environmentally friendly are on the raise for similar applications.

Recently, solid-state solar cells fabricated using carbon quantum dots derived from natural materials like chitin, glucose, chitosan, *etc*. are widely reported [109]. CQDs obtained from natural biomass or organic wastes were examined for being used in solar cells, as they showed both excitation-dependent/independent emission and also size-dependent fluorescence. Solar cells, when sensitized with such BCDs, displayed an improvement in conversion efficiency and the mechanism was found to be fluorescence quenching as proposed by Zhang *et al.* [110]. They proposed a mechanism for the enhancement of

fluorescent quenching using BCD derived from grass *viz.* The quenching of excited state photoelectron can happen by either an electron acceptor and/or an injection of the photoexcited electron into the conduction band. The latter principle can also be applied to enhance the efficiency of solar cells for other fluorescent quantum dots/nanodot sensitizers. Marinovic *et al*. [111] reported the preparation of CDs from various natural sources and used them as sensitizers for nanostructured solar cells based on TiO_2. After a careful investigation of the optical, structural and material properties of families of BCDs, they concluded that the efficiency of the solar cell in energy harvesting was very much influenced by the functional groups and especially, amino and carboxylic acid groups were highly beneficial in this regard.

Choi *et al.* [112] have reported the synthesis of a BCD-Ag hybrid system, where the BCD was carbon quantum dots prepared from α-cyclodextrin. This natural carbon dot, apart from acting as a reducing agent also behaved as a platform for the processing of polymer-based solar cells and polymer LEDs. The mechanism of operation was surface plasmon resonance, which ultimately resulted in enhanced absorption, significant radiative emission and enhanced current and luminescent efficiencies as polymer LEDs and as polymer solar cells, displaying a high-power conversion efficiency and almost 99% of internal quantum efficiency. Among LEDs, white LEDs (WLEDs) are recently being focused on more because of their characteristic emission, which covers a broad spectrum. They are also thermally stable and have a tunable fluorescence emission [113].

Electrochemical sensors: The usage of carbon quantum dots-based electrodes prepared from biomass is the material of recent research both for scientists and industrialists owing to their structural diversities, tuneable physical or chemical properties and economical, environmental and social considerations. Their porous structure, amicability for taking up heteroatoms, special physico-chemical properties and good electroconductivity make them able candidates for electrochemical energy storage. With a large surface area, they possess more specific sites, which allow the easy passage of electrolytes and hence accelerate reaction kinetics. A highly selective and sensitive carbon quantum dot derived from chia seeds, a natural precursor was reported as an electrochemical sensor for hydrazine by Sha *et al*. [114]. Another electroactive molecule of interest that was studied using N-doped CQD was dopamine. Recognized as a neuro-transmitter and a chemical messenger in the brain, levels of this molecule beyond permissible levels (10^{-8} to 10^{-6} M) may lead to severe neuro disorders and hence accurate and precise detection of dopamine becomes important for clinical purposes [115,116]. Jiang *et al.* [117] fabricated an N-doped CQD deposited on GCE (NCQD/GCE), which showed brilliant electrochemical properties and used this as a sensing tool to detect dopamine. A collated information of applications of doped BCDs used in various applications is provided in Table-2 [118]. Sources, methods of synthesis followed and quantum yield of the doped products are also provided.

Batteries: Batteries incorporating metal ions Li^+, Na^+, K^+, Al^{2+} and Zn^{2+} are the most recently explored ones [134]. Lithium

TABLE-2
APPLICATIONS OF DOPED AND CO-DOPED CARBON QUANTUM DOTS (CQDs)

Method of synthesis	Source/precursor	Doping element	Colour	Quantum yield (%)	Application	Ref.
Hydrothermal	Grass	N	Blue	2.5-6.2	Detection of Cu^{2+} ions	[119]
Hydrothermal	Glucose	N	Blue	0.7	White light emission	[120]
Hydrothermal	Dried monkey grass	N	Blue	0.7	Detection of I^-	[121]
Hydrothermal	Gingko leaf	N	Blue	22.8	Label-free detection of the drug salazosulfapyridine	[122]
Hydrothermal	Garlic	N, S	Blue	13	Detection of Fe^{3+} ions in lake and tap waters, in cell imaging	[123]
Hydrothermal	Casein	N, S	Blue	31.8	Detection of Hg^{2+} ions, bio thiols like l-cysteine, homocysteine and glutathione	[124]
Hydrothermal	Feathers, egg white, egg yolk and manure from pigeon	N, S	Blue	24.87, 17.48, 16.34 and 33.50	Detection of Hg^{2+}/and Fe^{3+} ions	[125]
Hydrothermal	Eleocharisdulcis juice	N, P	Navy blue	3.3	Anti-counterfeiting ink, Fe^{3+} ions detection	[126]
Acid base neutralization	Glucose	N, P	Green	9.59	Detection of curcumin and cell imaging	[127]
Acid carbonization	Sucrose	S	Blue	5.77	Detection of Fe^{3+} ions in acidic environment	[128]
Carbonization	Waste frying oil and sulphuric acid	S		3.66	Cell imaging (HeLa cell line)	[129]
Hydrothermal	Sucrose & phosphoric acid	P	Blue	21.8	Detection of explosive-TNT	[130]
Solvothermal	Lactose and phosphoric acid	P	Yellow	62	Detection of Al^{3+} and Zn^{2+} ions	[131]
Solvothermal	Citric acid	F	Yellow	31	Intracellular Ag^+ detection cell imaging studies.	[132]
Microwave	Citric acid, Urea, boric acid	B	Green	15	Non-linear optical applications	[133]

ions, the lightest metallic element is already established to have many electrochemical advantages like high energy density and voltage. It also works on a wide range of temperatures in the solid state as the small radius of the metal allows easy diffusion of solids.

Li-ion batteries: Glucose-derived carbon dots were used to replace the anodes in Li-ion batteries which resulted in a superior performance even after 500 cycles [135]. But the capacity was found to gradually decrease with increasing current density. This was attributed to a large number of Li^+ trapped in the initial cycles blocking the further transmission of Li ions from the electrode to the electrolyte. However, in the subsequent cycles, the deintercalation of Li ions was also reported due to the large interlayer spacing. Li batteries with anodes made from microporous algae carbon [136] and banana peel [137] were found to exhibit a high specific charge (445 mAh g^{-1} at 0.5 C) and high gravimetric capacity (1090 mAh g^{-1} at the current density of 50 mA g^{-1}). Nitrogen-doped electrodes obtained from garlic peel and egg yolk are also available in the literature [138,139]. With current densities of 1.0,2.0, 4.0 and 8.0 A g^{-1}, the garlic-derived one has achieved reversible capacities of 320, 290, 215 and 145 mAh g^{-1}, respectively. The presence of N in the carbon matrix of the anodic material is cited as the major reason for the reported capacities, which introduces mesoporous carbon structures rather than a disordered carbon structure and hence more embedded Li ions in the matrix. And the egg yolk-derived one is highly preferred for its high coulombic efficiency of 59.6% with a first discharge capacity of 1234 mAh g^{-1}, which is again due to the irreversible lithiation behaviour. Reduced overpotential and good cycling stability of Li-ion batteries have also been reported using CQDs derived from corn cob. In the case of Li-ion batteries, when $LiPF_6$ electrolytes were used with these naturally derived CQDs as additives, a nominal enhancement in specific discharge capacity was observed which indicated the possibility of these electrolyte additives contributing to the prevention of dendrites at the anode [140].

Zn ion batteries: Zinc ion batteries (ZIB) find potential applications in energy storage especially in harsh environments like aerospace, submarines and particularly with mild aqueous electrolytes. Interest was to design ZIB, which would withstand elevated temperatures and sub-zero conditions and hence was the arrival of Zn-air batteries [141]. Porous carbon obtained from soya beans, doped with nitrogen and functionalized with a sulphonic acid group was used as anode in the Zn-air battery. With a surface area of 844.0 m^2 g^{-1}, the specific capacitance was 174.4 F g^{-1} at a current density of 0.25 A g^{-1} and the capacity retention was reported as 65.6% at 2 A g^{-1}. The reported specific capacitance was found to be much higher when compared to the previously reported N-doped carbons but without functionalization [142].

Catalytic activity: Apart from high capacitance and coulombic efficiencies, reports on the activity of doped CQDs to catalyze ORR (oxidation reduction reaction) at the cathode is also available in the literature. The ORR at cathode is one of the stringent requirements in polymer electric fuel cells (PEFC) and metal-air batteries. Though Pt/C electrodes are used for this purpose, dual-doped CQDs are also emerging in this field. The effect of super capacitance as recorded by cyclic voltammetry shows an obvious characteristic peak corresponding to ORR activity (-0.25 V, -2.3 mA cm^{-2}) with O_2 saturation [143,144], which was absent in the case of N_2 saturation. Similar peaks of ORR activity for P, N-CQDs and S, N-CQDs were reported to be detected at -0.26 V (-2.0 mA cm^{-2}) and -0.28 V (-1.2 mA cm^{-2}), respectively. The reported current potential and peak activity of B, N -CQDs were found to be higher than that of P, N-CQDs and S, N-CQDs and also single doped CQDs. Thus, the dual doping of heteroatoms inducing a possible synergetic performance enhancement attributed to the enhancement of ORR activity of such CQDs was reported [145].

Miscellaneous applications: As discussed already, the BCDs possess extraordinary properties, which facilitate a number of biological applications like drug delivery, biological assays and bioimaging. Excellent biocompatibility, good stability and rapid cellular uptake tendency make them ideal candidates to execute drug loading release in biological systems. BCDs derived from *E. coli* [146], dried shrimp [147], pasteurized milk [29], *etc*. being fluorescent vectors are reported for their thera-peutic drug delivery studies.

Target bioimaging and therapy is another field in which BCDs have tremendous applications. In such studies, BCDs are used as highly efficient imaging agents for photoluminescent imaging of tumour cells. The latest progress in the development of CDs in targeted bioimaging and tumour treatment is reviewed by Shen *et al*. [148]. Ziyi *et al.* [149] have reported the synthesis of CDs from commercial beer and studied the cytotoxic properties. As no obvious cell inhibition at nominal concentrations was observed, they reported the beer-derived CDs as an effective nanocarrier for anticancer therapy and also as a safe material for bioimaging and image-guided drug delivery in cancer treatment. In addition to the above-discussed applications, CQDs derived from biomass have also other broad range of applications like light display materials, anticounter-feiting, confidential materials, fluorescent inks, *etc*. [150].

Conclusion

In this short review, we described different synthetic methods, characterization techniques and applications of plain and doped carbon quantum dots derived from natural biomass resources. The hydrothermal carbonization method was found to be ideal for the synthesis of doped and co-doped CQDs. The doping of heteroatoms to the carbon framework of the nanomaterial was found to enhance the properties and functionalities multifold, especially in electrochemical applications. The main applications of BCDs, such as optical sensing, electrochemical sensing, detection of pesticides and fungicides, electrochemiluminescence and electrocatalytic activities and their role in batteries and solar cells are reviewed. Even though considerable research has been carried out for developing new natural bioresources, innovative synthetic methods, extensive applications, materials, strategic designs and devices with improved performance and challenges are yet to be explored.

CONFLICT OF INTEREST

The authors declare that there is no conflict of interests regarding the publication of this article.

REFERENCES

1. K.J. Singh, T. Ahmed, P. Gautam, A.S. Sadhu, D.-H. Lien, S.-C. Chen, Y.-L. Chueh and H.-C. Kuo, *Nanomaterials*, **11**, 1549 (2021); https://doi.org/10.3390/nano11061549
2. J.H. Shen, Y.H. Zhu, C. Chen, X.L. Yang and C.Z. Li, *Chem. Commun.*, **47**, 2580 (2011); https://doi.org/10.1039/C0CC04812G
3. J. Lu, P.S.E. Yeo, C.K. Gan, P. Wu and K.P. Loh, *Nat. Nanotechnol.*, **6**, 247 (2011); https://doi.org/10.1038/nnano.2011.30
4. R. Liu, D. Wu, S. Liu, K. Koynov, W. Knoll and Q. Li, *Angew. Chem. Int. Ed.*, **48**, 4598 (2009); https://doi.org/10.1002/anie.200900652
5. H. Ming, Z. Ma, Y. Liu, K.M. Pan, H. Yu, F. Wang and Z.H. Kang, *Dalton Trans.*, **41**, 9526 (2012); https://doi.org/10.1039/c2dt30985h
6. M. Amjadi, T. Hallaj, H. Asadollahi, Z. Song, M. de Frutos and N. Hildebrandt, *Sensor Actust. Biol. Chem.*, **244**, 425 (2017); https://doi.org/10.1016/j.snb.2017.01.003
7. X.Y. Xu, R. Ray, Y. Gu, L. Ploehn, L. Gearheart, K. Raker and W.A. Scrivens, *J. Am. Chem. Soc.*, **126**, 12736 (2004); https://doi.org/10.1021/ja040082h
8. Y.Q. Zhang, D.K. Ma, Y. Zhuang, X. Zhang, W. Chen, L.L. Hong, Q.X. Yan, K. Yu and S.M. Huang, *J. Mater. Chem.*, **22**, 16714 (2012); https://doi.org/10.1039/c2jm32973e
9. L. Zheng, Y. Chi, Y. Dong, J. Lin and B. Wang, *J. Am. Chem. Soc.*, **131**, 4564 (2009); https://doi.org/10.1021/ja809073f
10. Z. Ma, H. Ming, H. Huang, Y. Liu and Z.H. Kang, *New J. Chem.*, **36**, 861 (2012); https://doi.org/10.1039/c2nj20942j
11. S. Liu, J.Q. Tian, L. Wang, Y.W. Zhang, X.Y. Qin, Y.L. Luo, A.M. Asiri, A.O. Al-Youbi and X. Sun, *Adv. Mater.*, **24**, 2037 (2012); https://doi.org/10.1002/adma.201200164
12. F. Wang, Z. Xie, H. Zhang, C.Y. Liu and Y.G. Zhang, *Adv. Funct. Mater.*, **21**, 1027 (2011); https://doi.org/10.1002/adfm.201002279
13. J. Chen, X. Wang, Y. Huang, S. Lv, X. Cao, J. Yun and D. Cao, *Eng. Sci.*, **5**, 30 (2019); https://doi.org/10.30919/es8d666
14. J. Di, J. Xia, X. Chen, M. Ji, S. Yin, Q. Zhang and H. Li, *Carbon*, **114**, 601 (2017); https://doi.org/10.1016/j.carbon.2016.12.030
15. T. Liu, J.X. Dong, S.G. Liu, N. Li, S.M. Lin, Y.Z. Fan, J.L. Lei, H.Q. Luo and N.B. Li, *J. Hazard. Mater.*, **322**, 430 (2017); https://doi.org/10.1016/j.jhazmat.2016.10.034
16. R. Zhang and W. Chen, *Biosens. Bioelectron.*, **55**, 83 (2014); https://doi.org/10.1016/j.bios.2013.11.074
17. D. Pooja, S. Saini, A. Thakur, B. Kumar, S. Tyagi and M.K. Nayak, *J. Hazard. Mater.*, **328**, 117 (2017); https://doi.org/10.1016/j.jhazmat.2017.01.015
18. H.-W. Chu, B. Unnikrishnan, A. Anand, Y.-W. Lin and C.-C. Huang, *J. Food Drug Anal.*, **28**, 539 (2020); https://doi.org/10.38212/2224-6614.1269
19. M. Lin, H.Y. Zou, T. Yang, Z.X. Liu, H. Liu and C.Z. Huang, *Nanoscale*, **8**, 2999 (2016); https://doi.org/10.1039/C5NR08177G
20. B.-C. Yin, B.-C. Ye, H. Wang, Z. Zhu and W. Tan, *Chem. Commun.*, **48**, 1248 (2012); https://doi.org/10.1039/C1CC15639J
21. H. Zhang, Y. Chen, M. Liang, L. Xu, S. Qi, H. Chen and X. Chen, *Anal. Chem.*, **86**, 9846 (2014); https://doi.org/10.1021/ac502446m
22. C. Tang, J. Zhou, Z. Qian, Y. Ma, Y. Huang and H. Feng, *J. Mater. Chem. B Mater. Biol. Med.*, **5**, 1971 (2017); https://doi.org/10.1039/C6TB03361J
23. P. Yuan and D.R. Walt, *Anal. Chem.*, **59**, 2391 (1987); https://doi.org/10.1021/ac00146a015
24. S. Chen, Y.L. Yu and J.H. Wang, *Anal. Chim. Acta*, **999**, 13 (2018); https://doi.org/10.1016/j.aca.2017.10.026
25. Q. Zhang, C. Zhang, Z. Li, J. Ge, C. Li, C. Dong and S. Shuang, *RSC Adv.*, **5**, 95054 (2015); https://doi.org/10.1039/C5RA18176C
26. C. Jiang, H. Wu, X. Song, X. Ma, J. Wang and M. Tan, *Talanta*, **127**, 68 (2014); https://doi.org/10.1016/j.talanta.2014.01.046
27. V. Sharma, P. Tiwari and S.M. Mobin, *J. Mater. Chem. B Mater. Biol. Med.*, **5**, 8904 (2017); https://doi.org/10.1039/C7TB02484C
28. X. Zhang, M. Jiang, N. Niu, Z. Chen, S. Li, S. Liu and J. Li, *ChemSusChem*, **11**, 11 (2018); https://doi.org/10.1002/cssc.201701847
29. J. Zhang, H. Wang, Y. Xiao, J. Tang, C. Liang, F. Li, H. Dong and W. Xu, *Nanoscale Res. Lett.*, **12**, 611 (2017); https://doi.org/10.1186/s11671-017-2369-1
30. Y. Zhou, Y. Liu, Y. Li, Z. He, Q. Xu, Y. Chen, J. Street, H. Guo and M. Nelles, *RSC Adv.*, **8**, 23657 (2018); https://doi.org/10.1039/C8RA03272F
31. L. Ding, X. Wang, J. Li, J. Huang and Z. Li, *J. Technol. Mater. Sci. Ed.*, **33**, 1546 (2018).
32. Y. Guo, L. Zhang, F. Cao and Y. Leng, *Sci. Rep.*, **6**, 35795 (2016); https://doi.org/10.1038/srep35795
33. C. Kang, Y. Huang, H. Yang, X.F. Yan and Z.P. Chen, *Nanomaterials*, **10**, 2316 (2020); https://doi.org/10.3390/nano10112316
34. V. Manikandan and N.Y. Lee, *Environ. Res.*, **212**, 113283 (2022); https://doi.org/10.1016/j.envres.2022.113283
35. L. Wang and H.S. Zhou, *Anal. Chem.*, **86**, 8902 (2014); https://doi.org/10.1021/ac502646x
36. L. Cui, X. Ren, M. Sun, H. Liu and L. Xia, *Nanomaterials*, **11**, 3419 (2021); https://doi.org/10.3390/nano11123419
37. H. Lu, C. Li, H. Wang, X. Wang and S. Xu, *ACS Omega*, **4**, 21500 (2019); https://doi.org/10.1021/acsomega.9b03198
38. C.L. Li, C.M. Ou, C.C. Huang, W.C. Wu, Y.P. Chen, T.E. Lin, L.C. Ho, C.W. Wang, C.C. Shih, H.C. Zhou, Y.C. Lee, W.F. Tzeng, T.J. Chiou, S.T. Chu, J. Cang and H.T. Chang, *J. Mater. Chem. B*, **2**, 4564 (2014); https://doi.org/10.1039/c4tb00216d
39. N. Wang, Y. Wang, T. Guo, T. Yang, M. Chen and J. Wang, *Biosens. Bioelectron.*, **85**, 68 (2014); https://doi.org/10.1016/j.bios.2016.04.089
40. G. Oza, K. Oza, S. Pandey, S. Shinde, A. Mewada, M. Thakur, M. Sharon and M. Sharon, *Fluorescence*, **25**, 9 (2015); https://doi.org/10.1007/s10895-014-1477-x
41. J. Zhang, Y. Yuan, G. Liang and S. H. Yu, *Adv. Sci.*, **2**, 1500002 (2015); https://doi.org/10.1002/advs.201500002
42. B. Yin, J. Deng, X. Peng, Q. Long, J. Zhao, Q. Lu, Q. Chen, H. Li, H. Tang, Y. Zhang and S. Yao, *Analyst*, **138**, 6551 (2013); https://doi.org/10.1039/C3AN01003A
43. W. Meng, X. Bai, B. Wang, Z. Liu, S. Lu and B. Yang, *Energy Environ. Materials*, **2**, 172 (2019); https://doi.org/10.1002/eem2.12038
44. W.B. Lu, X.Y. Qin, S. Liu, G.H. Chang, Y.W. Zhang, Y.L. Luo, A.M. Asiri, A.O. Al-Youbi and X.P. Sun, *Anal. Chem.*, **84**, 5351 (2012); https://doi.org/10.1021/ac3007939
45. Y. Liu, Y. Zhao and Y. Zhang, *Sens. Actuators B Chem.*, **196**, 647 (2014); https://doi.org/10.1016/j.snb.2014.02.053
46. P.K. Sarswat and M.L. Free, *Phys. Chem. Chem. Phys.*, **17**, 27642 (2015); https://doi.org/10.1039/C5CP04782J
47. X. Feng, Y. Jiang, J. Zhao, M. Miao, S. Cao, J. Fang and L. Shi, *RSC Adv.*, **5**, 31250 (2015); https://doi.org/10.1039/C5RA02271A
48. L. Janus, M. Piatkowski, J. Radwan-Praglowska, D. Bogdal and D. Matysek, *Nanomaterials*, **9**, 274 (2019); https://doi.org/10.3390/nano9020274
49. R. Atchudan, T.N. Edison, K.R. Aseer, S. Perumal, N. Karthik and Y.R. Lee, *Biosens. Bioelectron.*, **99**, 303 (2018); https://doi.org/10.1016/j.bios.2017.07.076
50. D. Gao, X. Liu, D. Jiang, H. Zhao, Y. Zhu, X. Chen, H. Luo, H. Fan and X. Zhang, *Sens. Actuators B Chem.*, **277**, 373 (2018); https://doi.org/10.1016/j.snb.2018.09.031

51. Z. Peng, Y. Zhou, C. Ji, J. Pardo, K.J. Mintz, R.R. Pandey, C.C. Chusuei, R.M. Graham, G. Yan and R.M. Leblanc, *Nanomaterials*, **10**, 1560 (2020); https://doi.org/10.3390/nano10081560
52. A. Saengsrichan, C. Saikate, P. Silasana, P. Khemthong, W. Wanmolee, J. Phanthasri, S. Youngjan, P. Posoknistakul, N. Laosiripojana, K.C.-W. Wu, S. Ratchahat and C. Sakdaronnarong, *Int. J. Mol. Sci.*, **23**, 5001 (2022); https://doi.org/10.3390/ijms23095001
53. Y. Yang, D. Huo, H. Wu, X. Wang, J. Yang, M. Bian, Y. Ma and C. Hou, *Sens. Actuators B Chem.*, **274**, 296 (2018); https://doi.org/10.1016/j.snb.2018.07.130
54. Q. Wang, X. Liu, L. Zhang and Y. Lv, *Analyst*, **137**, 5392 (2012); https://doi.org/10.1039/c2an36059d
55. R. Purbia and S. Paria, *Biosens. Bioelectron.*, **79**, 467 (2016); https://doi.org/10.1016/j.bios.2015.12.087
56. R. Liu, J. Zhang, M. Gao, Z. Li, J. Chen, D. Wu and P. Liu, *RSC Adv.*, **5**, 4428 (2015); https://doi.org/10.1039/C4RA12077A
57. J. Gong, X. An and X. Yan, *New J. Chem.*, **38**, 1376 (2014); https://doi.org/10.1039/C3NJ01320K
58. B. Tian, T. Fu, Y. Wan, Y. Ma, Y. Wang, Z. Feng and Z. Jiang, *J. Nanobiotechnology*, **19**, 456 (2021); https://doi.org/10.1186/s12951-021-01211-w
59. G. Dan, P. Zhang, L. Zhang, H. Liu, Z. Pu and S. Shang, *Opt. Mater.*, **8**, 272 (2018); https://doi.org/10.1016/j.optmat.2018.06.012
60. X. Liu, T. Li, Y. Hou, Q. Wu, J. Yi and G. Zhang, *RSC Adv.*, **6**, 11711 (2016); https://doi.org/10.1039/C5RA23081K
61. X. Qin, W. Lu, A.M. Asiri, A.O. Al-Youbi and X. Sun, *Sens. Actuators B Chem.*, **184**, 156 (2013); https://doi.org/10.1016/j.snb.2013.04.079
62. Y. Feng, D. Zhong, H. Miao and X. Yang, *Talanta*, **140**, 128 (2015); https://doi.org/10.1016/j.talanta.2015.03.038
63. V. Ramanan, S.K. Thiyagarajan, K. Raji, R. Suresh, R. Sekar and P. Ramamurthy, *ACS Sustain. Chem. Eng.*, **4**, 4724 (2016); https://doi.org/10.1021/acssuschemeng.6b00935
64. W.L. Ang, C.A.L. Boon Mee, N.S. Sambudi, A.W. Mohammad, C.P. Leo, E. Mahmoudi, M. Ba-Abbad and A. Benamor, *Sci. Rep.*, **10**, 21199 (2020); https://doi.org/10.1038/s41598-020-78322-1
65. C. Zhao, X. Li, C. Cheng and Y. Yang, *Microchem. J.*, **147**, 183 (2019); https://doi.org/10.1016/j.microc.2019.03.029
66. B. Zhi, M.J. Gallagher, B.P. Frank, T.Y. Lyons, T.A. Qiu, J. Da, A.C. Mensch, R.J. Hamers, Z. Rosenzweig, D.H. Fairbrother and C.L. Haynes, *Carbon*, **129**, 438 (2018); https://doi.org/10.1016/j.carbon.2017.12.004
67. H.J. Yashwanth, S.R. Rondiya, N.Y. Dzade, S.D. Dhole, D.M. Phase and K. Hareesh, *Vacuum*, **180**, 109589 (2020); https://doi.org/10.1016/j.vacuum.2020.109589
68. R. Zhang, Y.B. Liu, L. Yu, Z. Li and S.Q. Sun, *Nanotechnology*, **24**, 225601 (2013); https://doi.org/10.1088/0957-4484/24/22/225601
69. A. Sachdev and P. Gopinath, *Analyst*, **140**, 4260 (2015); https://doi.org/10.1039/C5AN00454C
70. X. Yang, Y. Zhuo, S. Zhu, Y. Luo, Y. Feng and Y. Dou, *Biosens. Bioelectron.*, **60**, 292 (2014); https://doi.org/10.1016/j.bios.2014.04.046
71. Y. Zhou, P.Y. Liyanage, D.L. Geleroff, Z. Peng, K.J. Mintz, S.D. Hettiarachchi, R.R. Pandey, C.C. Chusuei, P.L. Blackwelder and R.M. Leblanc, *ChemPhysChem*, **19**, 2589 (2018); https://doi.org/10.1002/cphc.201800248
72. Z. Gao, X. Wang, J. Chang, D. Wu, L. Wang, X. Liu, F. Xu, Y. Guo and K. Jiang, *RSC Adv.*, **5**, 48665 (2015); https://doi.org/10.1039/C5RA05365J
73. F. Ehrat, S. Bhattacharyya, J. Schneider, A. Löf, R. Wyrwich, A.L. Rogach, J.K. Stolarczyk, A.S. Urban and J. Feldmann, *Nano Lett.*, **17**, 7710 (2017); https://doi.org/10.1021/acs.nanolett.7b03863
74. N. Papaioannou, A. Marinovic, N. Yoshizawa, A.E. Goode, M. Fay, A. Khlobystov, M.M. Titirici and A. Sapelkin, *Sci. Rep.*, **8**, 6559 (2018); https://doi.org/10.1038/s41598-018-25012-8
75. M. Yoshikawa, Y. Mori, H. Obata, M. Maegawa, G. Katagiri, H. Ishida and A. Ishitani, *Appl. Phys. Lett.*, **67**, 694 (1995); https://doi.org/10.1063/1.115206
76. H. Liu, Y. Zhang and C. Huang, *J. Pharm. Anal.*, **9**, 127 (2019); https://doi.org/10.1016/j.jpha.2018.10.001
77. C.J. Reckmeier, J. Schneider, A.S. Susha and A.L. Rogach, *Opt. Express*, **24**, A312 (2016); https://doi.org/10.1364/OE.24.00A312
78. L. Tang, R. Ji, X. Cao, J. Lin, H. Jiang, X. Li, K.S. Teng, C.M. Luk, S. Zeng, J. Hao and S.P. Lau, *ACS Nano*, **6**, 5102 (2012); https://doi.org/10.1021/nn300760g
79. J. Peng, W. Gao, B.K. Gupta, Z. Liu, R. Romero-Aburto, L. Ge, L. Song, L.B. Alemany, X. Zhan, S.A. Vithayathil, B.A. Kaipparettu, G. Gao, A.A. Marti, T. Hayashi, J.-J. Zhu and P.M. Ajayan, *Nano Lett.*, **12**, 844 (2012); https://doi.org/10.1021/nl2038979
80. Y. Li, Y. Hu, Y. Zhao, G. Shi, L. Deng, Y. Hou and L. Qu, *Adv. Mater.*, **23**, 776 (2011); https://doi.org/10.1002/adma.201003819
81. Y. Xie, D. Cheng, X. Liu and A. Han, *Sensors*, **19**, 3169 (2019); https://doi.org/10.3390/s19143169
82. M.P. Sk, A. Jaiswal, A. Paul, S.S. Ghosh and A. Chattopadhyay, *Sci. Rep.*, **2**, 383 (2012); https://doi.org/10.1038/srep00383
83. B. De and N. Karak, *RSC Adv.*, **3**, 8286 (2013); https://doi.org/10.1039/c3ra00088e
84. A.B. Siddique, A.K. Pramanick, S. Chatterjee and M. Ray, *Sci. Rep.*, **8**, 9770 (2018); https://doi.org/10.1038/s41598-018-28021-9
85. M. Jorns and D. Pappas, *Nanomaterials*, **11**, 1448 (2021); https://doi.org/10.3390/nano11061448
86. S. Safranko, D. Goman, A. Stankovic, M. Medvidovic-Kosanovic, T. Moslavac, I. Jerkovic and S. Jokic, *Chemosensors*, **9**, 138 (2021); https://doi.org/10.3390/chemosensors9060138
87. Y. Guo, L. Zhang, S. Zhang, Y. Yang, X. Chen and M. Zhang, *Biosens. Bioelectron.*, **63**, 61 (2015); https://doi.org/10.1016/j.bios.2014.07.018
88. P. Lv, Y. Yao, H. Zhou, J. Zhang, Z. Pang, K. Ao, Y. Cai and Q. Wei, *Nanotechnology*, **28**, 165502 (2017); https://doi.org/10.1088/1361-6528/aa6320
89. J. Jana, M. Ganguly, K.R.S. Chandrakumar, G. Mohan Rao and T. Pal, *Langmuir*, **33**, 573 (2017); https://doi.org/10.1021/acs.langmuir.6b04100
90. R. Bao, Z. Chen, Z. Zhao, X. Sun, J. Zhang, L. Hou and C. Yuan, *Nanomaterials*, **8**, 386 (2018); https://doi.org/10.3390/nano8060386
91. W. Zou, X. Ma and P. Zheng, *Cellulose*, **27**, 2099 (2020); https://doi.org/10.1007/s10570-019-02926-8
92. Y.S. Xia and C.-Q. Zhu, *Talanta*, **75**, 215 (2007); https://doi.org/10.1016/j.talanta.2007.11.008
93. C. Wang, C. Wang, P. Xu, A. Li, Y. Chen and K. Zhuo, *J. Mater. Sci.*, **51**, 861 (2016); https://doi.org/10.1007/s10853-015-9410-5
94. J.R. Bhamore, S. Jha, R.K. Singhal, T.J. Park and S.K. Kailasa, *J. Mol. Liq.*, **264**, 9 (2018); https://doi.org/10.1016/j.molliq.2018.05.041
95. Z. Ramezani, M. Qorbanpour and N. Rahbar, *Colloids Surf. A Physicochem. Eng. Asp.*, **549**, 58 (2018); https://doi.org/10.1016/j.colsurfa.2018.04.006
96. N. Architha, M. Ragupathi, C. Shobana, T. Selvankumar, P. Kumar, Y.S. Lee and R.K. Selvan, *Environ. Res.*, **199**, 111263 (2021); https://doi.org/10.1016/j.envres.2021.111263
97. H. Xu, X. Yang, G. Li, C. Zhao and X. Liao, *J. Agric. Food Chem.*, **63**, 6714 (2015); https://doi.org/10.1021/acs.jafc.5b02319
98. Z. Han, H. Zhang, L. He, S. Pan, H. Liu and X. Hu, *Microchem. J.*, **146**, 300 (2019); https://doi.org/10.1016/j.microc.2019.01.024
99. Y. Song, X. Yan, Z. Li, L. Qu, C. Zhu, R. Ye, S. Li, D. Du and Y. Lin, *J. Mater. Chem. B Mater. Biol. Med.*, **6**, 3181 (2018); https://doi.org/10.1039/C8TB00116B
100. W. Wang, Y.C. Lu, H. Huang, A.J. Wang, J.R. Chen and J.J. Feng, *J. Biosens. Bioelectron.*, **64**, 517 (2015); https://doi.org/10.1016/j.bios.2014.09.066

101. Q. Zhang, J. Liang, L. Zhao, Y. Wang, Y. Zheng, Y. Wu and L. Jiang, *Front. Chem.*, **8**, 665 (2020); https://doi.org/10.3389/fchem.2020.00665
102. Y. Yang, D. Huo, H. Wu, X. Wang, J. Yang, M. Bian, Y. Ma and C. Hou, *Sens. Actuators B Chem.*, **274**, 296 (2018); https://doi.org/10.1016/j.snb.2018.07.130
103. H. Li, C. Sun, R. Vijayaraghavan, F. Zhou, X. Zhang and D.R. MacFarlane, *Carbon*, **104**, 33 (2016); https://doi.org/10.1016/j.carbon.2016.03.040
104. R.J. Forster, P. Bertoncello and T.E. Keyes, *Annu. Rev. Anal. Chem.*, **2**, 359 (2009); https://doi.org/10.1146/annurev-anchem-060908-155305
105. M.M. Richter, *Chem. Rev.*, **104**, 3003 (2004); https://doi.org/10.1021/cr020373d
106. J.D. Luttmer and A.J. Bard, *J. Electrochem. Soc.*, **126**, 414 (1979); https://doi.org/10.1149/1.2129054
107. C. Venkateswara Raju and S. Senthil Kumar, *Chem. Commun.*, **53**, 6593 (2017); https://doi.org/10.1039/C7CC03349D
108. B. Sun, H. Qi, F. Ma, Q. Gao, C. Zhang and W. Miao, *Anal. Chem.*, **82**, 5046 (2010); https://doi.org/10.1021/ac9029289
109. J. Briscoe, A. Marinovic, M. Sevilla, S. Dunn and M. Titirici, *Angew. Chem. Int. Ed.*, **54**, 4463 (2015); https://doi.org/10.1002/anie.201409290
110. H. Zhang, Y. Wang, P. Liu, Y. Li, H.G. Yang, T. An, P.-K. Wong, D. Wang, Z. Tang and H. Zhao, *Nano Energy*, **13**, 124 (2015); https://doi.org/10.1016/j.nanoen.2015.01.046
111. A. Marinovic, L.S. Kiat, S. Dunn, M.-M. Titirici and J. Briscoe, *ChemSusChem*, **10**, 1004 (2017); https://doi.org/10.1002/cssc.201601741
112. H. Choi, S.-J. Ko, Y. Choi, P. Joo, T. Kim, B.R. Lee, J.W. Jung, H.J. Choi, M. Cha, J.R. Jeong, I.-W. Hwang, M.H. Song, B.-S. Kim and J.Y. Kim, *Nat. Photonics*, **7**, 732 (2013); https://doi.org/10.1038/nphoton.2013.181
113. S. Yang, P. He, T. Yuan, Y. Li, X. Li, Y. Zhang, L. Fan, Y. Shi and T. Meng, *Nanoscale*, **12**, 4826 (2020); https://doi.org/10.1039/C9NR10958G
114. R. Sha, S. Jones, N. Vishnu, B. Soundiraraju, and S. Badhulika, *Electroanalysis*, **30**, 2228 (2018); https://doi.org/10.1002/elan.201800255
115. J. Kim, M. Jeon, K. Paeng and I. Paeng, *Anal. Chim. Acta*, **619**, 87 (2008); https://doi.org/10.1016/j.aca.2008.02.042
116. N. Speed, J. Heinrich, M. Kennedy, R. Vaughan, J. Javitch, S. Russo, C. Lindsley, K. Niswender and A. Galli, *ACS Chem. Neurosci.*, **1**, 476 (2010); https://doi.org/10.1021/cn100031t
117. G. Jiang, T. Jiang, H. Zhou, J. Yao and X. Kong, *RSC Adv.*, **5**, 9064 (2015); https://doi.org/10.1039/C4RA16773B
118. G. Kandasamy, *J. Carbon Res. C.*, **5**, 24 (2019); https://doi.org/10.3390/c5020024
119. S. Liu, J. Tian, L. Wang, Y. Zhang, X. Qin, Y. Luo, A.M. Asiri, A.O. Al-Youbi and X. Sun, *Adv. Mater.*, **24**, 2037 (2012); https://doi.org/10.1002/adma.201290148
120. S. Dey, P. Chithaiah, S. Belawadi, K. Biswas and C.N.R. Rao, *J. Mater. Res.*, **29**, 383 (2014); https://doi.org/10.1557/jmr.2013.295
121. H. Zhang, Y. Li, X. Liu, P. Liu, Y. Wang, T. An, H. Yang, D. Jing and H. Zhao, *Environ. Sci. Technol. Lett.*, **1**, 87 (2013); https://doi.org/10.1021/ez400137j
122. X. Jiang, D. Qin, G. Mo, J. Feng, C. Yu, W. Mo and B. Deng, *J. Pharm. Biomed. Anal.*, **164**, 514 (2019); https://doi.org/10.1016/j.jpba.2018.11.025
123. Y. Chen, Y. Wu , B. Weng, B. Wang and C. Li, *Sens. Actuators B Chem.*, **223**, 689 (2016). https://doi.org/10.1016/j.snb.2015.09.081
124. S. Xu, Y. Liu, H. Yang, K. Zhao, J. Li and A. Deng, *Anal. Chim. Acta*, **964**, 150 (2017); https://doi.org/10.1016/j.aca.2017.01.037
125. Q. Ye, F. Yan, Y. Luo, Y. Wang, X. Zhou and L. Chen, *Spectrochim. Acta A Mol. Biomol. Spectrosc.*, **173**, 854 (2017); https://doi.org/10.1016/j.saa.2016.10.039
126. R. Bao, Z. Chen, Z. Zhao, X. Sun, J. Zhang, L. Hou and C. Yuan, *Nanomaterials*, **8**, 386 (2018); https://doi.org/10.3390/nano8060386
127. Y. Liu, X. Gong, W. Dong, R. Zhou, S. Shuang and C. Dong, *Talanta*, **183**, 61 (2018); https://doi.org/10.1016/j.talanta.2018.02.060
128. V.M. Naik, D.B. Gunjal, A.H. Gore, S.P. Pawar, S.T. Mahanwar, P.V. Anbhule and G.B. Kolekar, *Diam. Relat. Mater.*, **88**, 262 (2018); https://doi.org/10.1016/j.diamond.2018.07.018
129. Y. Hu, J. Yang, J. Tian, L. Jia and J.S. Yu, *Carbon*, **77**, 775 (2014); https://doi.org/10.1016/j.carbon.2014.05.081
130. D. Shi, F. Yan, T. Zheng, Y. Wang, X. Zhou and L. Chen, *RSC Adv.*, **5**, 98492 (2015); https://doi.org/10.1039/C5RA18800H
131. K.M. Omer and A.Q. Hassan, *Microchim. Acta*, **184**, 2063 (2017); https://doi.org/10.1007/s00604-017-2196-1
132. G. Zuo, A. Xie, J. Li, T. Su, X. Pan and W. Dong, *J. Phys. Chem. C*, **121**, 26558 (2017). https://doi.org/10.1021/acs.jpcc.7b10179
133. A.B. Bourlinos, G. Trivizas, M.A. Karakassides, A. Kouloumpis, M. Baikousi, D. Gournis, A. Bakandritsos, K. Hola, O. Kozak, R. Zboril, I. Papagiannouli, P. Aloukos and S. Courisef, *Carbon*, **83**, 173 (2015); https://doi.org/10.1016/j.carbon.2014.11.032
134. D. Chao, W. Zhou, F. Xie, C. Ye, H. Li, M. Jaroniec and S.-Z. Qiao, *Sci. Adv.*, **6**, eaba4098 (2020); https://doi.org/10.1126/sciadv.aba4098
135. H. Yang, S. Ye, J. Zhou and T. Liang, *Front Chem.*, **7**, 274 (2019); https://doi.org/10.3389/fchem.2019.00274
136. H. Ru, N. Bai, K. Xiang, W. Zhou, H. Chen and X.S. Zhao, *Electrochim. Acta*, **194**, 10 (2016); https://doi.org/10.1016/j.electacta.2016.02.083
137. E.M. Lotfabad, J. Ding, K. Cui, A. Kohandehghan, W.P. Kalisvaart, M. Hazelton and D. Mitlin, *ACS Nano*, **8**, 7115 (2014); https://doi.org/10.1021/nn502045y
138. V. Selvamani, R. Ravikumar, V. Suryanarayanan, D. Velayutham and S. Gopukumar, *Electrochim. Acta*, **190**, 337 (2016); https://doi.org/10.1016/j.electacta.2016.01.006
139. S. Wang, H. Wang, R. Zhang, L. Zhao, X. Wu, H. Xie, J. Zhang and H. Sun, *J. Alloys Compd.*, **746**, 567 (2018); https://doi.org/10.1016/j.jallcom.2018.02.293
140. P. Arumugam, S.R. Elumali, K. Raman, S. A.M, T. Purushotham and R. SubashChandrabose, *ECS Trans.*, **107**, 16547 (2022); https://doi.org/10.1149/10701.16547ecst
141. C.C. Yang and S.J. Lin, *J. Power Sources*, **112**, 497 (2002); https://doi.org/10.1016/S0378-7753(02)00438-X
142. C. Zhao, G. Liu, N. Sun, X. Zhang, G. Wang, Y. Zhang, H. Zhang and H. Zhao, *Chem. Eng. J.*, **334**, 1270 (2018); https://doi.org/10.1016/j.cej.2017.11.069
143. R. Liu, D. Wu, X. Feng and K. Müllen, *Angew. Chem. Int. Ed.*, **49**, 2565 (2010); https://doi.org/10.1002/anie.200907289
144. W. Yang, T.P. Fellinger and M. Antonietti, *J. Am. Chem. Soc.*, **133**, 206 (2011); https://doi.org/10.1021/ja108039j
145. Y. Han, D. Tang, Y. Yang, C. Li, W. Kong, H. Huang, Y. Liu and Z. Kang, *Nanoscale*, **7**, 5955 (2015); https://doi.org/10.1039/C4NR07116F
146. V.N. Mehta, S.S. Chettiar, J.R. Bhamore, S.K. Kailasa and R.M. Patel, *J. Fluoresc.*, **27**, 111 (2017); https://doi.org/10.1007/s10895-016-1939-4
147. S.L. D'Souza, B. Deshmukh, J.R. Bhamore, K.A. Rawat, N. Lenka and S.K. Kailasa, *RSC Adv.*, **6**, 12169 (2016); https://doi.org/10.1039/C5RA24621K
148. C.-L. Shen, H.-R. Liu, Q. Lou, F. Wang, K.-K. Liu, L. Dong and C.-X. Shan, *Theranostics*, **12**, 2860 (2022); https://doi.org/10.7150/thno.70721
149. Z. Wang, H. Liao, H. Wu, B. Wang, H. Zhao and M. Tan, *Anal. Methods*, **20**, 8911 (2015); https://doi.org/10.1039/C5AY01978H
150. T.C. Wareing, P. Gentile and A.N. Phan, *ACS Nano*, **15**, 15471 (2021); https://doi.org/10.1021/acsnano.1c03886